Classification of GNSS SNR Data for Different Environments and Satellite Orbital Information

Rameez UR Rahman Lighari, Markus Berg, Erkki T. Salonen, Aarno Parssinen
Centre for Wireless Communications – Radio Technology Research Unit, University of Oulu, Finland
rameez.lighari@oulu.fi

***Abstract*—In this paper, a data classification method for analyzing the aspects of Signal-to-Noise Ratio (SNR) for Global Navigation Satellite System (GNSS) in real conditions is introduced. Different parts of measured environments and the orbital information of satellites are used as criteria for data classification. It consists of: 1) taking fish eye images of measured routes; 2) dividing measured environments into four potential sub environments (*open area, forest area, single building blockage, and street canyon*); 3) classifying satellites into nine different groups as function of elevation angles; and 4) creating a table containing the information of mean and standard deviation of SNR for different environments and satellite elevation angles. Results show good correlation of SNR's between same sub environments for different satellite elevation ranges which offer useful insight to regenerate a generalized set of SNR parameters in the laboratory environment for the development of 3D GNSS channel model.**

***Index Terms*—GNSS, measurements, data classification, satellite communication.**

I. Introduction

Lately, Global Navigation Satellite System (GNSS) or more commonly Global Positioning System (GPS) receivers have become a must have feature in mobile phones and multipurpose wearable device. They are likewise being used in material logistic systems, automobile (burglary assurance), and transport tracking systems. GPS can measure the geographical location of a user's receiver anywhere on earth with the accuracy up to 1 meter. However, the presence of multipath signals especially in urban areas, and the position of satellites can have serious impacts on the positioning accuracy of a GPS device.

In order to guarantee an acceptable user experience, GNSS receiver's location accuracy needs to be proven cautiously on the grounds of interference, sensitivity, and use cases in various surroundings and in different atmospheric conditions. Therefore, the performance evaluation of GNSS devices in 3D laboratory measurement environment is gaining increasing interest among scientific community and device manufacturers. Additionally, bringing the time consuming, costly, and uncontrollable field tests in to a controllable laboratory environment gives cost savings and speeds up the product development.

Some of previous investigations have used 3D city models to improve the accuracy of GNSS receiver by detecting non-line-of-sight (NLOS) signals for Land Mobile Satellite (LMS) channel in urban canyons [1]–[3]. However, 3D maps of cities are hard to come by and also, the polarization of multipath components is not taken into account. GNSS laboratory measurement environments are also marketed by companies, e.g. ETS-Lindgren [4] and Keysight Technologies [5]. Despite the provided reference setups for GNSS over-the-air (OTA) testing, publicly available measurement results and channel models are not available from these companies.

This paper is based on the recent measurement campaign performed with polarization based measurement system for the development of 3D channel model [6]. Both Right Hand Circularly Polarized (RHCP) and Left Hand Circularly Polarized (LHCP) antennas are employed to obtain direct and reflected signals simultaneously. As the result of measurements, characteristics of polarization based reflections, position error, coverage efficiency (i.e. mean number of tracked satellites), and the impact of satellite elevation angle on received Signal-to-Noise Ratio (SNR) for a typical multipath environment are investigated in [7] to create a dynamic channel model for the laboratory environment.

In this paper, we present data classification approach based on classification of measured environments into four sub environments, orbital information of satellites, and video recording of environments with fish-eye lens. The method of using fish-eye lens to track the environment first time appeared in one of the earlier papers on GNSS in mid 1990s [8]. The data classification method, with inputs of video recording and GPS signal measures, is accordingly designed to output SNR distributions and look up table containing the mean and standard deviation of SNR for sub environments at different satellite elevation angles. By applying the proposed method to data collected in different environments, an analysis of SNR in real conditions is provided, and SNR parameters between sub environments are compared as function of satellite elevation angle, which will provide useful insight for the development of 3D GNSS channel model.

The rest of paper is organized as follows. We present brief description of measurement setup in section II. Next, the measured environments are introduced in section III. Third, the data classification approach and results are presented in section IV. Finally, relevant conclusions are drawn based on the results in section V.

This research is supported by the Finnish Funding Agency for Innovation (Tekes) through the Hilla research program and Centre for Wireless Communications.

(a) University Campus Area

(b) Suburban Residential Area

(c) Urban Downtown Area

Fig. 1: Aerial view of measured environments in Oulu, Finland.

II. Measurement Setup

The measurement system consists of two GNSS receivers, capable of recording signals that are transmitted by various constellations of satellites (GPS, GLONASS, and Beidou). For this paper, only GPS signals were recorded using RHCP (sensitive for line-of-sight component and a double reflected component) and LHCP (sensitive for first order reflections) antennas. In addition to video recording continuous images with fish-eye lens were taken to track the changing environment. The camera was held head-high pointing towards zenith. During the test, both receivers collected GPS satellite data at a rate of 1Hz including the Coordinated Universal Time (UTC), received SNR, number of satellites tracked and used in position fix, and the orbital information of each visible satellite (i.e. satellite elevation, and azimuth). A detailed description of the measurement setup along with antenna orientations is presented earlier [6].

III. Environments

The mentioned GPS data were collected for three different environments; consisting of, university campus, suburban residential, and urban downtown areas. Starting position of all three measured routes was nearly an open-sky area to obtain complete GPS ephemeris and good position fix. Measurements were made in Oulu, Finland during the months, when the trees were with and without leaves, respectively. Measurements for university campus area represent the case in which the trees were with leaves and measurements for suburban residential, and urban downtown areas represent the case when deciduous trees were almost without leaves. Fig. 1 shows the aerial view of three environments.

A. University Campus Area

The measurement route included a typical campus area environment with built-up area, narrow street canyons, walkways, canopy of metal over the walkway, and a small forest area. The total length of the route is 1 km. The test vehicle took about 10 min to finish the trajectory and about 650 data points are recorded by GNSS receivers.

B. Suburban Residential Area

The measured route consist of a typical residential area occupied primarily by private residences. The measured route included trees surrounding the roads, two storey houses with wooden structures, narrow streets, and a three storey office building located nearly 30 meters away from the measured route. The total length of the route is 1.1 km. The test vehicle took about 10 min to finish the trajectory and about 720 data points are recorded by GNSS receivers.

C. Urban Downtown Area

A heavily dense area with many businesses, recreations, narrow streets, underpass, and tall buildings close together. The subway (underpass) underneath the roads and railway lines is roughly 80 meters long. The total length of the route is 1.4 km. The test vehicle took about 13 min to finish the trajectory and about 850 data points are recorded by GNSS receivers.

IV. Data Classification

Based on the measurements from various environments shown in Fig. 1, the different parts of each environment and the orbital information of satellites are used as criterion for data classification. Each measured environment is further divided into four different environments: (1) open area; (2) forest area; (3) single building blockage; and (4) street canyon. Classification of satellites is based on their elevation, however in case of single building blockage azimuth information of satellites is also taken into account. An elevation mask of 10° is used for the forest area due to insufficient data and visibility of satellites below 10°, and the tall building structures of street canyon prevented visibility of satellites for all elevations below 30°.

A. Notations

Elevation and azimuth angles of satellite are represented by θ_S and ϕ_S, respectively and, similarly, the elevation tilt angles of directional receiver antennas are presented with θ_{RHCP} and θ_{LHCP}. Environments consisting of university campus, and suburban residential areas are presented with U_{CA}, and S_{RA}, respectively. Merged SNR data from different

sub environments are denoted by M_d. In single building case, Blocked side of building is represented by B, whereas, the other (open) side is presented with O. Finally, the mean and standard deviation of SNR are represented by μ_{SNR}, and σ_{SNR}.

B. Approach

Fig. 2 represents the flow chart of the data classification approach. After the route selection and measurement setup, the selected route is measured with GNSS receivers in parallel with a video camera to track the continuously changing environment.

The first and the foremost important step in data classification is to synchronize the clocks between National Marine Electronics Association (NMEA) data and video recording. Now, by the means of video recording each environment is classified into four different environments as mentioned above in section IV.

Then, satellites are classified in nine different groups based on their elevation and the data form all the satellites that fall in same group are merged together. In the next step, elevation based data are sorted for each sub environment.

The same process is repeated for each environment and data from each sub environment are merged together. Finally, a table is created containing the information of mean and standard deviation of SNR for different environments and elevation ranges.

However, in the case of single building blockage satellites are classified into two different classes (1) blocked by building (180° in ϕ_S); and (2) other side which we refer as line-of-sight (LOS) situation (180° in ϕ_S) as illustrated in Fig 3.

C. Results

In order to get the full coverage for both upper and lower hemisphere, measurements were performed at different antenna orientations (i.e. θ_{RHCP} and θ_{LHCP}). However, in this paper the results are presented for $\theta_{RHCP} = \theta_{LHCP} = 45°$. More details about different antenna orientations can be found in [6], [7]. Furthermore, It should be noted that there was no area in measured environments open enough to be considered as an open area. Also, during the measurement campaign no satellites between the elevation angles of 81°– 90° were received because of the northern location of the measurement routes. For the deeper investigation two different operation environments were selected where mean and variance of the Left Hand (LH) and Right Hand (RH) SNR values are plotted as a function of elevation angles.

Bar charts of the μ_{SNR} and σ_{SNR} from the forest area (as described under Data Classification) for RHCP antenna are shown in Figs. 4 and 5. The small difference between the μ_{SNR} and σ_{SNR} values from two environments might be due to lack of leaves in suburban residential area. In general, the merged data from two environments gives a better prospect of tree shadowing effect. Similar kind of behavior is observed for different sub environments (e.g. single building blockage and street canyon). Therefore, the rest of results are based on merged data from each sub environment instead of data from individual environments.

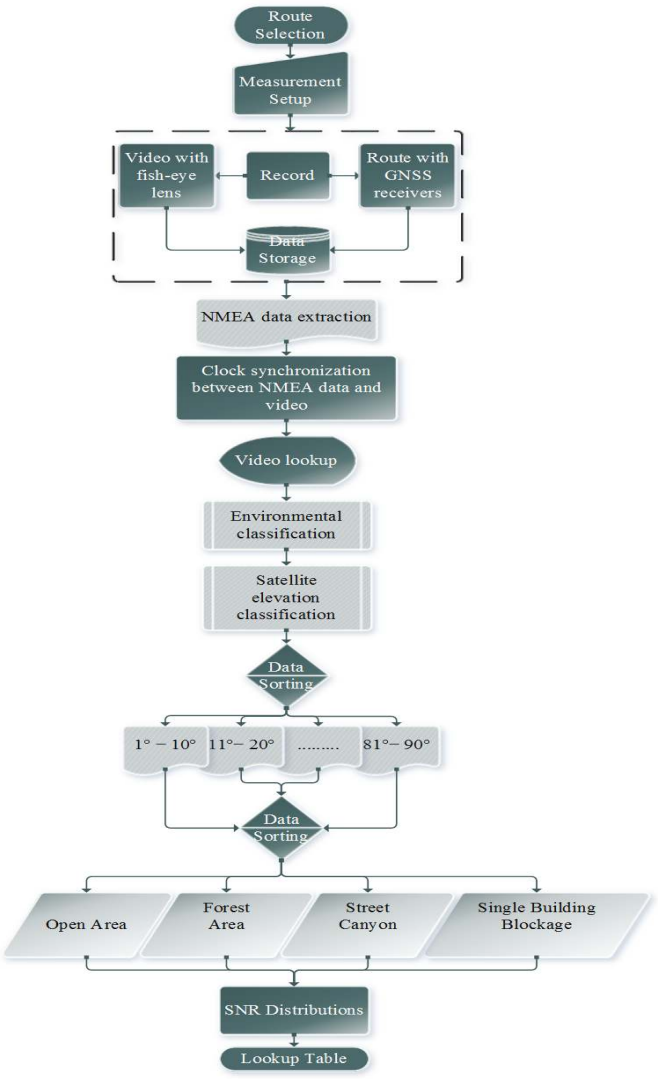

Fig. 2: Flow chart of data classification approach.

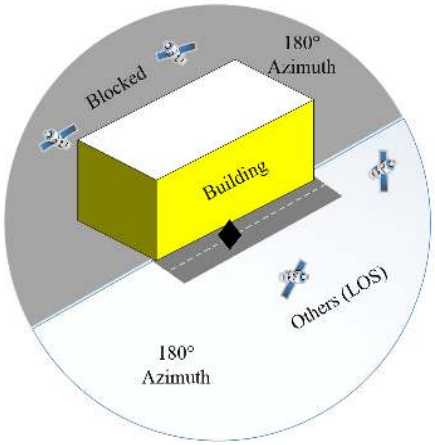

Fig. 3: Case of single building blockage.

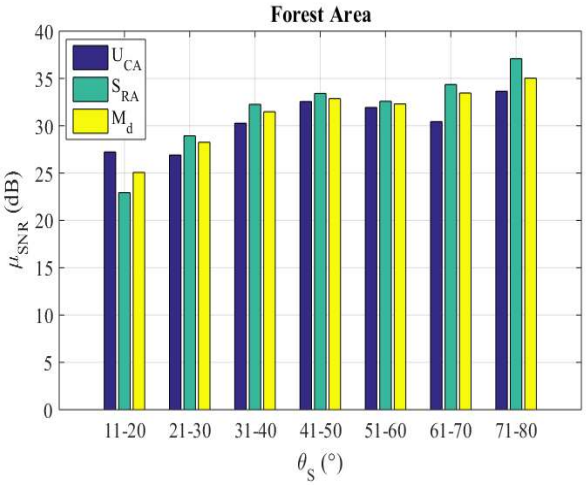

Fig. 4: Comparison of μ_{SNR} between environments for RHCP.

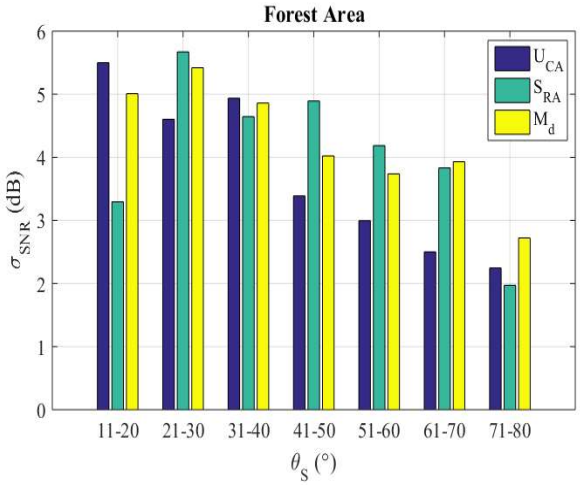

Fig. 5: Comparison of σ_{SNR} between environments for RHCP.

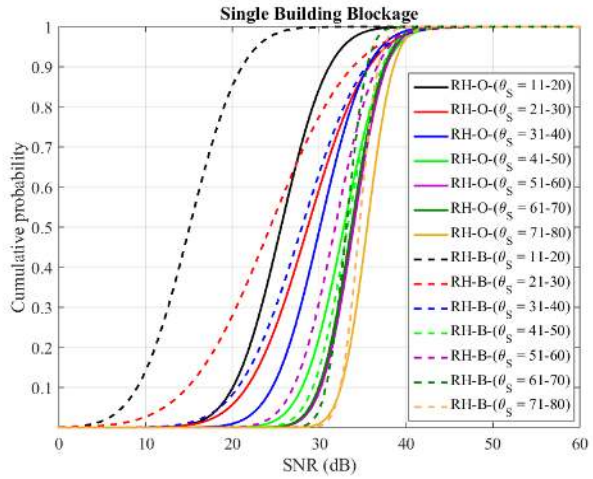

Fig. 6: Cumulative probability distributions of SNR for RHCP.

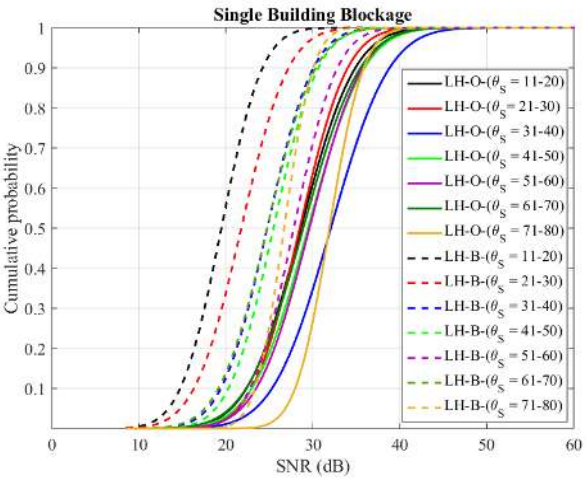

Fig. 7: Cumulative probability distributions of SNR for LHCP.

Shown in Figs. 6 and 7 are the cumulative probability distributions of SNR for single building blockage. For RH (Fig. 6) most satellites are shadowed by building and satellites on opposite to buildings have higher values. RH levels of satellites on both sides of building tends to increase with increase in θ_S and RH values are closely matched at higher θ_S. Higher LH values (Fig. 7) of other satellites suggest stronger reflection from the building and lower values are due weaker reflections from shadowed satellites.

The results of cumulative probability distributions of SNR (RH and LH) for street canyon are presented in Fig 8. At lower θ_S, RH and LH levels are closely matched and pointing towards stronger reflections and weak LOS condition. However, at higher θ_S, RH has LOS situation and lower levels of LH pointing towards weaker reflections from ground below.

An increasing trend in mean SNR values can be observed for all sub environments for RHCP antenna as presented in Table I. Furthermore, at higher θ_S mean values are closely matched pointing towards LOS situation. On the other hand, at lower θ_S, LH–SNR's are either closely matched or higher than RH–SNR's as reported in Table II.

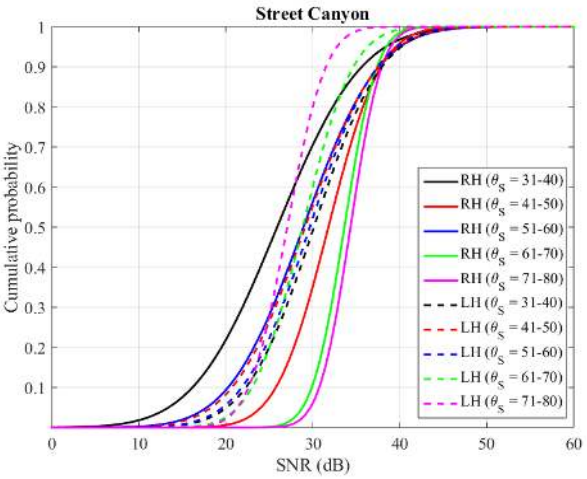

Fig. 8: Comparison of SNR distribution between RHCP and LHCP.

Overall decreasing pattern can be seen in the values of

TABLE I: MEAN AND STANDARD DEVIATION OF RHCP SNR

θ_S	Forest Area		Single Building (Blocked)		Single Building (Others)		Street Canyon	
	μ_{SNR}	σ_{SNR}	μ_{SNR}	σ_{SNR}	μ_{SNR}	σ_{SNR}	μ_{SNR}	σ_{SNR}
01° – 10°	–	–	–	–	–	–	–	–
11° – 20°	25.06	5.01	15.06	4.70	25.59	4.32	–	–
21° – 30°	28.25	5.41	24.34	7.42	28.67	5.48	–	–
31° – 40°	31.48	4.85	28.01	5.75	30.08	4.28	25.90	7.59
41° – 50°	32.87	4.02	33.26	3.11	32.83	3.75	31.79	4.71
51° – 60°	32.30	3.73	31.82	3.75	33.94	2.92	28.92	6.75
61° – 70°	33.46	3.92	33.13	1.83	33.70	2.92	33.64	2.92
71° – 80°	35.02	2.72	34.611	1.69	35.52	2.35	34.33	2.79
81° – 90°	–	–	–	–	–	–	–	–

TABLE II: MEAN AND STANDARD DEVIATION OF LHCP SNR

θ_S	Forest Area		Single Building (Blocked)		Single Building (Others)		Street Canyon	
	μ_{SNR}	σ_{SNR}	μ_{SNR}	σ_{SNR}	μ_{SNR}	σ_{SNR}	μ_{SNR}	σ_{SNR}
01° – 10°	–	–	–	–	–	–	–	–
11° – 20°	22.97	4.12	19.49	3.68	28.63	4.88	–	–
21° – 30°	23.69	4.27	21.78	4.24	28.50	4.30	–	–
31° – 40°	25.13	3.52	24.76	4.14	32.07	5.27	30.13	6.09
41° – 50°	25.48	3.53	25.47	4.02	29.46	5.04	29.16	6.55
51° – 60°	23.90	4.40	27.82	3.91	29.61	4.76	29.65	6.09
61° – 70°	23.13	3.98	24.75	4.35	28.90	5.11	28.84	4.53
71° – 80°	24.79	3.15	26.71	2.59	31.91	3.06	27.06	3.46
81° – 90°	–	–	–	–	–	–	–	–

variance for both RH and LH in Table I and II. Variance values are widely spread at lower θ_S and at higher θ_S, values are closely distributed for both RH and LH.

V. CONCLUSION

In this article we have presented a data classification method based on the measurements from various environments. Different parts of each environment and the orbital information of satellites are used as criterion for data classification. First, the method involves taking fish eye images of measured routes and analyzing the images to divide each environment into four potential sub environments: (1) open area; (2) forest area; (3) single building blockage; and (4) street canyon. Then, satellites are classified in nine different groups based on their elevation and the data form all the satellites that fall in same group are merged together. Finally, a table is created containing the information of mean and standard deviation of SNR for different environments and elevation ranges.

The main drawback of this approach is the tedious and precise work required to classify data into sub environments if the area to be covered is extended: the process is only automated to limited extend. However, in the future more automatic pattern recognition of the still images could offer a faster way for SNR evaluation in different environments.

The results obtained with significant amount of data from three different environments showed good correlation of SNR between same sub environments. This information will be used to regenerate a generalized set of SNR parameters in the laboratory environment for 3D GNSS channel model.

Future efforts will include taking second round of measurements with 2nd generation measurement system equipped with dual polarized GPS antennas [9], and 360 degree images of environments. In addition to three environments described in this paper open and offshore areas will be measured separately.

REFERENCES

[1] A. Bourdeau, M. Sahmoudi, and J.-Y. Tourneret, "Tight Integration of GNSS and a 3D City Model for Robust Positioning in Urban Canyons," in *2012, ION GNSS*, USA, September 2012.

[2] E. Takeuchi, M. Yamazaki, K. Ohno, and S. Tadokoro, "GPS Measurement Model with Satellite Visibility using 3D map for Particle Filter," in *2011, International Conference on Robotics and Biomimetics (ROBIO)*, Phuket, Thailand, December 2011.

[3] K. A. B. Ahmad, M. Sahmoudi, C. Macabiau, A. Bourdeau, and G. Moura, "Reliable GNSS Positioning in Mixed LOS/NLOS Environments Using a 3D Model," in *2013, European Navigation Conference (ENC)*, 2013.

[4] M. D. Foegelle, and R. Borsato, "A-GPS Over-The-Air Test Method: Business and Technology Implications," *2009, White Paper*, [online], Available: http://www.ets-lindgren.com/WhitePaper-ETSL0709 (Accessed: September 20, 2016).

[5] Keysight Technologies, "A-GPS OTA Measurements," *2015*, [online], Available: http://literature.cdn.keysight.com/litweb/pdf/5990-6043EN.pdf (Accessed: September 20, 2016).

[6] M. Berg, R. Lighari, J. Kallankari, V. Majava, A. Parssinen, and E. T. Salonen, "Polarization Based Measurement System for Analysis of GNSS Multipath Signals," in *2016, 10th European Conference on Antennas and Propagation (EuCAP)*, Davos, Switzerland, April 2016.

[7] R. Lighari, M. Berg, J. Kallankari, A. Parssinen, and E. T. Salonen, "Analysis of the Measured RHCP and LHCP GNSS Signals in Multipath Environment," in *2016, 6th International Conference on Localization and GNSS (ICL-GNSS)*, Barcelona, Spain, June 2016.

[8] R. Akturan, and W. J. Vogel, "Photogrammetric Mobile Satellite Service Prediction," *Electron. Lett.*, vol. 31, no. 3, pp. 165–166, Feb. 1995.

[9] M. Berg, R. Lighari, T. Tuovinen, and E. T. Salonen, "Circularly Polarized GPS Antenna for Simultaneous LHCP and RHCP Reception with High Isolation," in press *2016, Loughborough Antennas and Propagation Conference (LAPC)*, Loughborough, UK, November 2016.